nature climate change

LETTERS

PUBLISHED ONLINE: 2 NOVEMBER 2015 | DOI: 10.1038/NCLIMATE2840

Atlantic-induced pan-tropical climate change over the past three decades

Xichen Li[1]*, Shang-Ping Xie[1]*, Sarah T. Gille[1] and Changhyun Yoo[2]

During the past three decades, tropical sea surface temperature (SST) has shown dipole-like trends, with warming over the tropical Atlantic and Indo-western Pacific but cooling over the eastern Pacific. Competing hypotheses relate this cooling, identified as a driver of the global warming hiatus[1,2], to the warming trends in either the Atlantic[3,4] or Indian Ocean[5]. However, the mechanisms, the relative importance and the interactions between these teleconnections remain unclear. Using a state-of-the-art climate model, we show that the Atlantic plays a key role in initiating the tropical-wide teleconnection, and the Atlantic-induced anomalies contribute ~55–75% of the tropical SST and circulation changes during the satellite era. The Atlantic warming drives easterly wind anomalies over the Indo-western Pacific as Kelvin waves and westerly anomalies over the eastern Pacific as Rossby waves. The wind changes induce an Indo-western Pacific warming through the wind–evaporation–SST effect[6,7], and this warming intensifies the La Niña-type response in the tropical Pacific by enhancing the easterly trade winds and through the Bjerknes ocean dynamical processes[8]. The teleconnection develops into a tropical-wide SST dipole pattern. This mechanism, supported by observations and a hierarchy of climate models, reveals that the tropical ocean basins are more tightly connected than previously thought.

The tropics have experienced marked climate change since 1979 when the era of global satellite observations began. SST trends exhibit a pan-tropical dipole-like pattern (Fig. 1a), with extensive warming from the tropical Atlantic to the Indo-western Pacific, and a triangular cooling pattern in the central–eastern Pacific. This tropical-wide gradient in the SST trend interacts with the atmospheric and oceanic circulation throughout the tropics (Fig. 1c,e), with an enhanced Walker circulation[9–11] and a La Niña-like Pacific subsurface response. These changes further contribute to global climate change[1,12,13] through multiple atmospheric teleconnections[8,14].

The tropical ocean basins are connected through an atmospheric bridge[15] into an interactive system. On interannual timescales, El Niño/Southern Oscillation (ENSO) dominates the tropical inter-basin teleconnections[15,16], although the Indian[17,18] and Atlantic[19–21] oceans experience regional effects that can feed back to the Pacific. In this inter-basin teleconnection, El Niño warming heats the Indian and Atlantic basins[13]. Were the same relationship to hold on multi-decadal timescales, the cooling of the eastern Pacific would be linked to decreased SSTs in the Indian and Atlantic basins (Supplementary Fig. 1), contrary to the observed trends. This discrepancy implies that other mechanisms are required to compensate the eastern Pacific-induced tropical cooling.

The north and tropical Atlantic has experienced a continuous warming trend, due to the combined effects of anthropogenic radiative forcing[7,22] and the change in meridional overturning circulation[23,24]. Pioneering studies using slab ocean–atmospheric models[3] and reduced-gravity ocean–atmospheric models[4] suggest that this observed Atlantic warming directly contributes to the eastern Pacific cooling, although the full range of ocean dynamics and atmospheric–ocean interactions may not be well represented by these idealized oceanic models. Here we simulate the global impact of the tropical Atlantic warming using a fully coupled Earth system model, and further investigate the mechanisms of these teleconnections using a hierarchy of climate models. The results from the coupled model show that the Atlantic warming can induce a basin-scale warming over the Indian Ocean and western Pacific through the atmospheric bridge. This secondary Indo-western Pacific warming, together with the original Atlantic warming, intensifies the easterly wind anomaly over the Pacific, accelerates the Walker circulation, and contributes to the La Niña-type response over the Pacific (Fig. 1). Both surface heat fluxes and ocean dynamics play key roles in this tropical-wide pattern formation.

We first test the hypothesis that the tropical Atlantic warming drives the tropical-wide change by nudging the tropical Atlantic SST in a state-of-the-art fully coupled model (Fig. 1b), the Community Earth System Model (CESM1, see Methods). The restoring reproduces the bulk of the observed warming trend over the tropical Atlantic (97%, see grey bars in Supplementary Fig. 2c). Forced by this Atlantic warming, the model (Fig. 1b) captures the detailed features of the observed tropical-wide SST changes (Fig. 1a), that is, a significant warming anomaly over the Indo-western Pacific (Supplementary Fig. 2c blue bars), and significant cooling anomalies in the off-equatorial eastern Pacific (purple and green bars). A Mann–Kendall test indicates that the observed equatorial Pacific cooling trend from 1979 to 2013 is only marginally significant (left red bar) owing to high internal variability and the short period. With a large sample size, the Pacific cooling is significant in the ensemble simulation with a Student t-test. In addition, the 25-year-mean results for each of the 12 ensemble members (Supplementary Fig. 2c) show a cooled equatorial eastern Pacific in response to the Atlantic warming, indicating a robust anti-correlated relationship between these two ocean basins. The coupled simulation captures 55–75% of the observed trends over the Indian and Pacific oceans, highlighting the association between the Atlantic warming and pan-tropical SST changes, although additional mechanisms, for example, anthropogenic radiative forcing for the Indo-western Pacific warming[7], are likely to be required to explain the entire observed SST trend.

The Atlantic warming-induced tropical-wide SST pattern drives a series of tropical climate changes in the CESM (Fig. 1 right panels). The enhanced convection forced by the surface warming heats the troposphere, and the deep convection over the Indo-western Pacific warm pool area intensifies the Indo-Pacific Walker circulation (Fig. 1c,d). At the surface, this circulation change manifests itself as

[1]Scripps Institution of Oceanography, University of California, San Diego, California 92093, USA. [2]Department of Atmospheric Science and Engineering, Ewha Womans University, Seoul 03760, Republic of Korea. *e-mail: xichenslc@gmail.com; sxie@ucsd.edu

© 2016 Macmillan Publishers Limited. All rights reserved

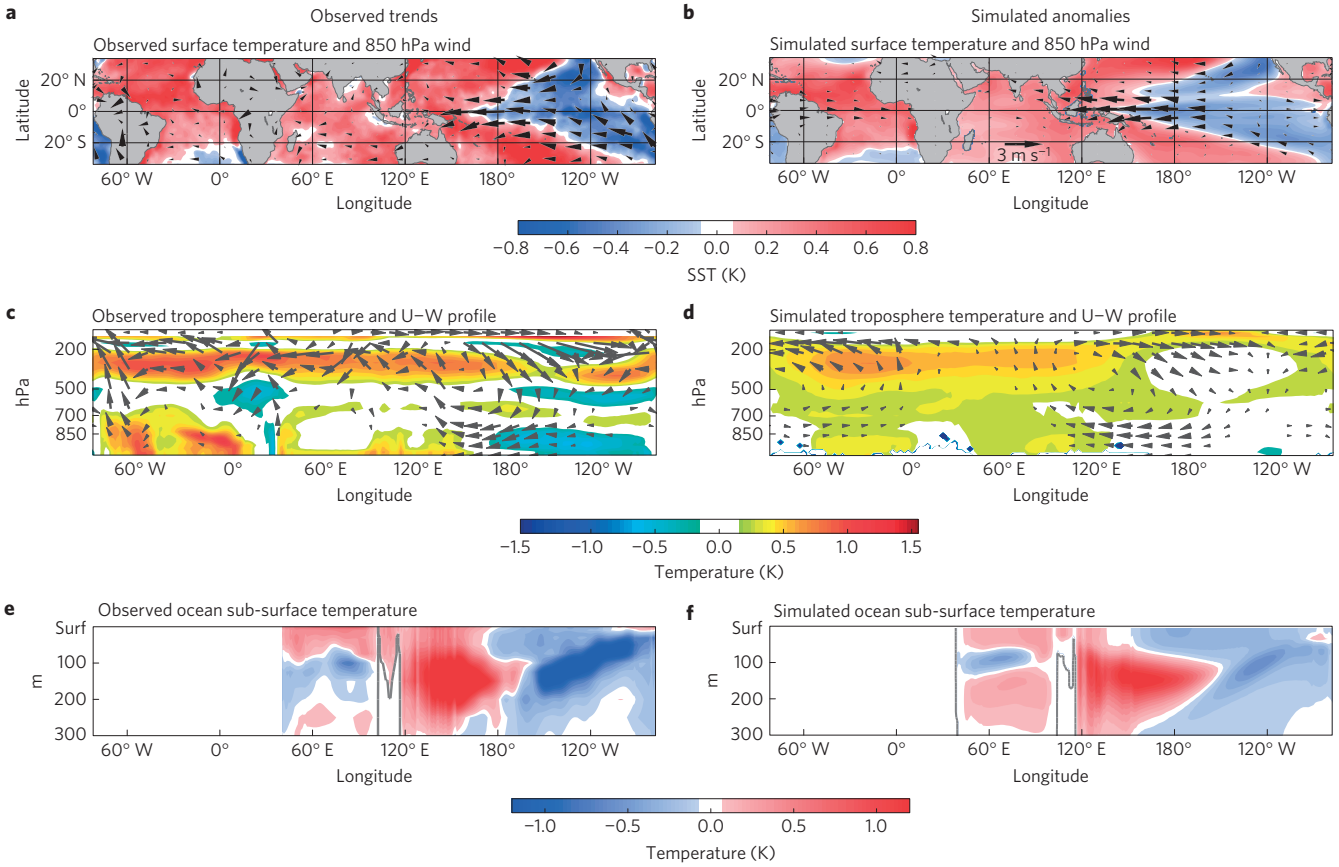

Figure 1 | Comparison of observed tropical climate changes with CESM coupled model simulation forced by the observed tropical-Atlantic-only SST changes. a,**b**, The observed (**a**) and simulated (**b**) SST changes (background colour) and 850 hPa wind anomaly (arrows) both exhibit a pan-tropical dipole SST change, with warming extending from the tropical Atlantic to the Indian Ocean and the western Pacific, and cooling over the central–eastern Pacific. The observed trends (**a**) are estimated using the Sen's slope method, from 1979 to 2012. **c**,**d**, The observed (**c**) and simulated (**d**) Walker circulation changes (arrows) and troposphere temperature anomalies (colour shading): the Indo-Pacific Walker circulation is enhanced. The vertical velocity is magnified by a factor of 750 to make its scale comparable to that of zonal wind. **e**,**f**, The observed (**e**) and simulated (**f**) ocean subsurface temperature anomalies (colour shading) for the tropical cross-section between 5° S and 5° N.

a strengthened easterly wind anomaly[11] over the equatorial Pacific (Fig. 1a). With the dynamical ocean–atmosphere coupling, this simulated equatorial Pacific easterly wind anomaly captures 68% of the observed trend (Supplementary Fig. 2c), albeit with a slight westward shift (Fig. 1b). This wind anomaly is accompanied by a La Niña-like Pacific subsurface anomaly both in observations and in the simulation (Fig. 1e,f). The coupled model successfully captures the main features of the observed temperature and circulation changes over the tropical ocean and atmosphere, although some of the detailed characteristics are not fully reproduced. In particular, the observed atmospheric temperature has exhibited a cooling trend over the African continent (Fig. 1b), associated with a downwelling flow in the troposphere. This is not well represented by the simulation, indicating that land–air interaction may be important for understanding the changes over that region. Additionally, the simulated atmospheric vertical motion (Fig. 1d) is both weaker and more widespread than the observed changes (Fig. 1c), which may be related to the convective scheme in the atmospheric model.

To better identify the potential sources of the pan-tropical climate variability (Fig. 1a), we also nudge the SST changes over the Indian Ocean and the Pacific Ocean, separately. The Indian Ocean nudging replicates the observed cooling trend in the eastern Pacific[1], albeit with a smaller amplitude, but it erroneously cools the Atlantic (Supplementary Fig. 3). The Pacific nudging, on the other hand, cools the Indian Ocean. Both simulations produce an SST response that is partially inconsistent with observations, indicating that the Atlantic is the most consistent driver of the pan-tropical dipole-like SST variability.

Although our Atlantic nudging simulations successfully reproduce the observed trends, the coupled model alone does not reveal the mechanisms underlying these pan-tropical inter-basin teleconnections. Next, we use an idealized atmospheric model and a comprehensive atmospheric model to identify the dynamical pathways by which the tropical Atlantic warming forces the tropical-wide climate changes.

CESM simulations involve both atmospheric dynamics and atmosphere–ocean interactions. To single out the immediate atmospheric responses to the Atlantic SST forcing, we introduce a tropical Atlantic heating to an idealized atmospheric model—the dry dynamical core of the GFDL atmospheric model (Methods). The atmospheric deep convection generated by the Atlantic warming (Supplementary Fig. 4) excites an equatorial Kelvin wave, inducing strong easterly wind anomalies to the east of the SST forcing (Supplementary Fig. 5b), as well as two Rossby wave packets with equatorial westerly wind anomalies and two off-equatorial cyclonic flows, west of the heat source. This circulation pattern closely resembles the classic Gill model[25]. Within one week, the Kelvin-wave-induced easterly wind anomalies extend from the Atlantic Ocean to the international Date Line (Supplementary Fig. 5c), traversing the entire Indian Ocean and western Pacific, whereas the Rossby-wave equatorial westerly wind anomalies occupy the eastern Pacific and Central America.

© 2016 Macmillan Publishers Limited. All rights reserved

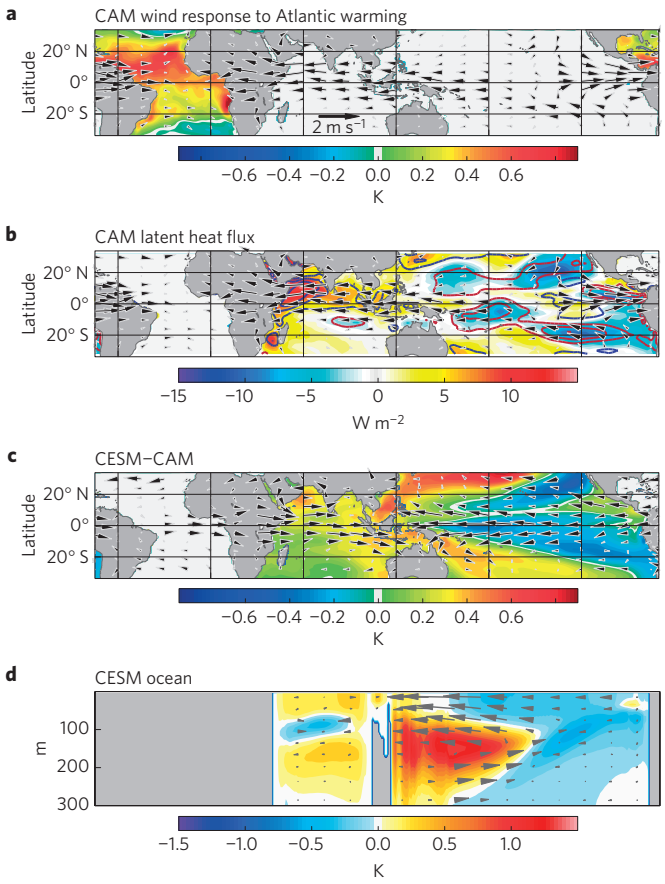

Figure 2 | Physical pathway for the Atlantic warming to drive tropical-wide SST changes. a, The Atlantic SST forcing and 850 hPa wind responses in CAM4. Deep convection forced by the tropical Atlantic warming induces convergent flows over the entire tropical region; that is, easterly wind anomalies over the Indo-western Pacific and westerly wind anomalies over the eastern Pacific. **b**, The wind changes in CAM4 further reduce the surface wind speed (blue contours) over vast areas of the Indian Ocean, suppress evaporation, and thus reduce the latent heat flux (red/yellow shading) from the ocean to the atmosphere (equivalent to a heating in the ocean). They also increase the surface wind speed (red contours) over much of the off-equatorial eastern Pacific and thus increase latent heat flux (blue shading) there. **c**, CESM–CAM4 differences in SST and 850 hPa wind. The anomalous Atlantic warming heats the Indo-western Pacific and cools the eastern Pacific. This SST gradient generates a secondary atmospheric circulation change, characterized by an enhanced easterly wind anomaly over the Pacific, and a westerly wind anomaly over the Atlantic–Indian oceans. **d**, Subsurface temperature and ocean current responses in CESM (the vertical velocity is magnified by 4,000 times). The easterly wind anomaly further drives the ocean surface current, strengthens the equatorial undercurrent and generates a La Niña-like ocean dynamical response. Processes shown in **c** and **d** interact with each other through the Bjerknes feedback.

Moisture processes are important in the tropics but are absent in the GFDL dry dynamical core. The Community Atmospheric Model (CAM4, Methods) is the atmospheric component of CESM1 and includes interactive moist processes. The CAM4 response agrees well with that of the idealized simulation (Supplementary Fig. 5c,d), again showing an easterly wind anomaly extending from the Atlantic to the Indo-western Pacific and a westerly wind anomaly over the eastern Pacific. The Kelvin-wave-induced easterly wind anomalies favour a La Niña-type ocean dynamical response[8], consistent with the coupled model results. In contrast, the Rossby-wave-induced westerly wind anomalies favour an El Niño-type response.

To investigate the direct ocean response to these atmospheric circulation anomalies, we use the anomalies to force an ocean-only model (POP2, see Supplementary Fig. 6). In the absence of ocean–atmosphere feedbacks, the ocean model response is different from the La Niña-type responses simulated in the fully coupled model. This discrepancy highlights the importance of atmosphere–ocean interactions in the pan-tropical teleconnections. The remainder of this work investigates atmosphere–ocean interactions that further enhance the equatorial Pacific easterly wind anomalies and the Walker circulation, thus contributing to a La Niña-like Pacific response.

Atmospheric forcing may influence regional SST by changing surface heat flux and oceanic dynamical effects[6,7]. In CAM4, the surface energy exchanges over the Indo-Pacific oceans are dominated by the wind-induced latent heat flux (Fig. 2b), whose contribution is ~3 times greater than that of all the other components of surface heat flux combined (Supplementary Fig. 7). The Kelvin-wave-induced easterly wind anomaly over the Indian Ocean reduces surface wind speed (blue contours in Fig. 2b) and suppresses evaporation, which warms the equatorial-northern Indian Ocean (red colour in Fig. 2b) through the wind–evaporation–SST effect[6] (WES, Methods). Note that in the atmosphere-only simulation (Fig. 2b), the SSTs are fixed and cannot feed back to the atmospheric circulation. The simulated regional-mean latent heat flux anomaly is ~4.35 W m^{-2}, corresponding to an initial heating rate of the ocean mixed layer of ~0.05 K per month, which implies a fast response of the Indo-western Pacific with a timescale of ~1 yr. This fast response is well reproduced in the coupled model and is supported by the statistical analyses of the observational data and the CMIP5 simulations (Supplementary Fig. 8).

To the west of the Atlantic warming, the Rossby-wave-induced circulation changes strengthen the trade winds and cool the off-equatorial eastern Pacific in both hemispheres (blue colour in Fig. 2b). This cooling signal may propagate equatorward and westward to the central-equatorial Pacific through the WES seasonal footprinting mechanism[26]. The Kelvin-wave-induced easterly wind anomaly also cools the central-equatorial Pacific around the international Date Line. These WES cooling effects contribute to an SST decrease over the central–eastern Pacific, which has been well simulated by a recent study using a slab ocean–atmosphere coupled model[3].

The Atlantic-induced Indo-western Pacific warming generates a secondary atmospheric deep convection (Fig. 2c, also see Supplementary Fig. 9) with westerly wind anomalies over the Indian Ocean, and an easterly wind anomaly across the Pacific basin. This secondary circulation change, representing an enhanced Indo-Pacific Walker circulation, explains the different atmospheric circulation responses between the CAM4 and CESM results. It reinforces the Atlantic-induced easterly wind anomalies over the western equatorial Pacific, overwhelming the Atlantic-induced westerly wind anomalies over the eastern equatorial Pacific. Atmospheric circulation changes further interact with Pacific Ocean dynamics through the Bjerknes feedback[4,8]. This feedback is at work in the coupled model (Fig. 2d): over the equatorial Pacific strong easterly winds drive an enhanced SST gradient, which further intensifies the winds, ultimately giving rise to a La Niña-like subsurface anomaly in the Pacific Ocean. In contrast, the ocean dynamical response is comparatively weak in the Indian Ocean, which experiences an overall warming in the upper 300 m with a cooling at ~100 m (Fig. 1e). The Indian Ocean temperature change is primarily a direct response to the surface heat fluxes, although the Indonesian throughflow may also contribute to these upper layer changes[27].

In summary, we have shown that the tropical Atlantic warming over the past three decades, aided by coupled ocean–atmosphere

© 2016 Macmillan Publishers Limited. All rights reserved

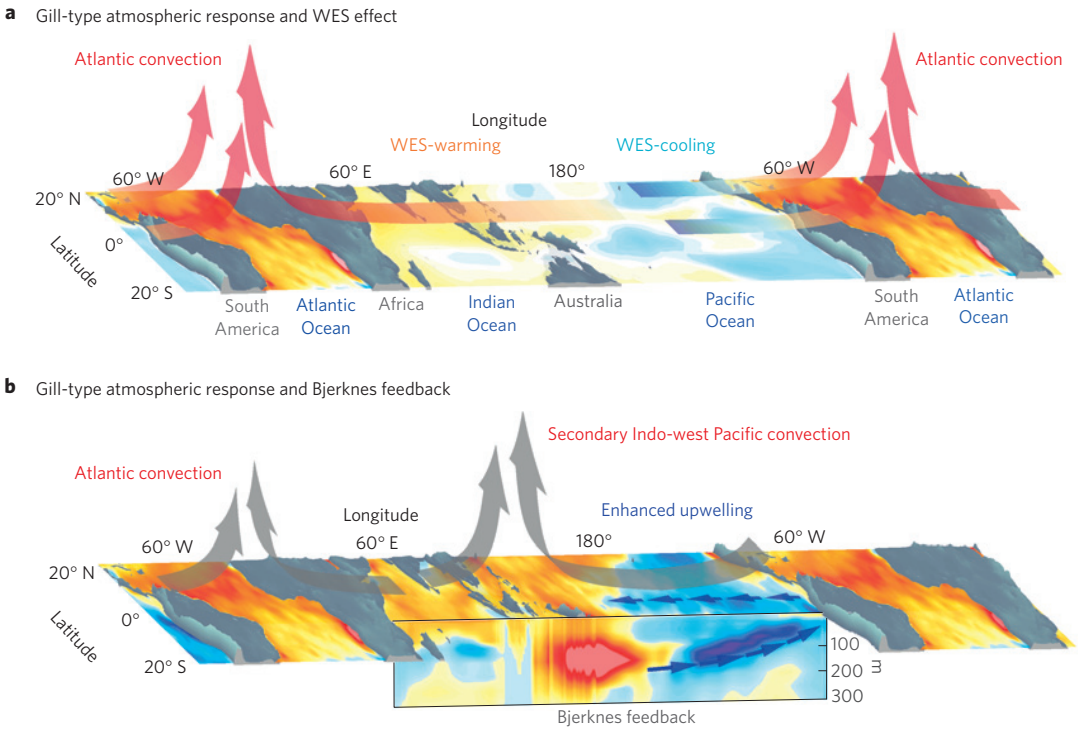

Figure 3 | Schematic graph of the physical mechanism. a, Atlantic warming generates anomalous atmospheric deep convection, mimicking the Gill convective model[28]. The deep convection forces an easterly wind anomaly over the Indian Ocean that suppresses local evaporation and increases the SST there. This is accompanied by a Rossby-wave-induced wind anomaly of opposing sign, which cools the eastern Pacific. This atmosphere–ocean surface interaction initiates a temperature gradient over the Indo-Pacific oceans. **b**, The Pacific Ocean dynamic effect positively feeds back on this SST gradient; that is, the SST gradient generates a secondary deep convection over the Indo-western Pacific warm pool, reinforcing the easterly wind anomalies over the Pacific basin, which intensifies the Ekman pumping over the eastern Pacific and enhances the Pacific undercurrent. These dynamical effects cool the eastern Pacific and warm the western Pacific, forming a positive feedback. The vertical cross-section in **b** illustrates the temperature and circulation anomalies in the subsurface Indo-Pacific.

processes, caused a tropical-wide response that included the Indo-western Pacific warming and eastern Pacific cooling. The direct atmospheric response to the tropical Atlantic warming includes easterly wind anomalies over the Indo-western Pacific in the form of Kelvin waves, and westerly wind anomalies over the eastern equatorial Pacific as Rossby waves (Fig. 3a), in line with Gill's solution. The easterly wind anomalies cause the Indo-western Pacific to warm and the central equatorial Pacific to cool through the WES effect, whereas the Rossby wave gyres intensify the easterly trade winds in the off-equatorial eastern Pacific, contributing to the equatorial Pacific cooling through the WES footprinting mechanism (Fig. 3a). This surface atmospheric–ocean interaction generates a temperature gradient over the Indo-Pacific basins, which further enhances the Walker circulation and induces easterly wind anomalies across the equatorial Pacific, and drives it into a La Niña state (Fig. 3b). The Bjerknes feedback helps amplify the coupling of the equatorial Pacific cooling and easterly intensification.

A global SST pattern characterized by the eastern Pacific cooling and warming over the rest of the oceans is identified as the most predictable mode at multi-year lead times[28]. Pacific decadal variability may be partly tied to Atlantic Multi-decadal Oscillation[29,30]. The tropical Atlantic warming trend is likely to be due to radiative forcing[7,22] and Atlantic Multi-decadal Oscillation[23,24], the latter possibly tied to the Atlantic meridional overturning circulation (AMOC). The mechanism revealed by this study suggests that the AMOC may force the pan-tropical decadal variability, and the slow timescales of the AMOC may explain the decadal predictability[19,28] of the tropical-wide SST pattern.

The Indo-western Pacific SST response to the tropical Atlantic warming is almost immediate, with a timescale of ~1 yr. In contrast, there exists a ~10 yr phase lag between the Atlantic warming and the cooling phase of the Pacific Decadal Oscillation[30]. This decadal-scale phase lag may be related to shorter-term variability such as ENSO, which serves as a stochastic forcing to the long-term variability. In this study we mainly focus on explaining the observed trend during the satellite era, but we plan to address this phase-lag problem in future work. Additionally, our coupled simulations are forced by a fixed radiative forcing. The radiative forcing changes caused by increased greenhouse gases could further warm the Atlantic Ocean and the Indo-western Pacific, although the impact of radiative forcing on the eastern Pacific requires further investigations.

Although recent studies of the global warming hiatus have focused on the Pacific effect[1], consistent with earlier studies[2–4] our results suggest that the hiatus may ultimately be traced back to the warming in the tropical Atlantic. This teleconnection is aided by Indo-western Pacific adjustments as revealed in this study. Together, these studies show that the three tropical ocean basins are linked more closely than previously thought, and on decadal timescales the tropical oceans should be considered as a single entity. In addition to the well-known ENSO-induced tropical-wide response that is dominant on interannual timescales, this study highlights the role of the tropical Atlantic in initiating a different pan-tropical dipole pattern that is important on decadal timescales.

Methods

Methods and any associated references are available in the online version of the paper.

Received 19 May 2015; accepted 24 September 2015; published online 2 November 2015

© 2016 Macmillan Publishers Limited. All rights reserved

References

1. Kosaka, Y. & Xie, S. P. Recent global-warming hiatus tied to equatorial Pacific surface cooling. *Nature* **501,** 403–407 (2013).
2. Meehl, G. A. *et al.* Model-based evidence of deep-ocean heat uptake during surface-temperature hiatus periods. *Nature Clim. Change* **1,** 360–364 (2011).
3. McGregor, S. *et al.* Recent Walker circulation strengthening and Pacific cooling amplified by Atlantic warming. *Nature Clim. Change* **4,** 888–892 (2014).
4. Kucharski, F. I. S., Kang, R. F. & Laura, F. Tropical Pacific response to 20th century Atlantic warming. *Geophys. Res. Lett.* **38,** L03702 (2011).
5. Luo, J. J., Sasaki, W. & Masumoto, Y. Indian Ocean warming modulates Pacific climate change. *Proc. Natl Acad. Sci. USA* **109,** 18701–18706 (2012).
6. Xie, S. P. & Philander, S. G. H. A coupled ocean-atmosphere model of relevance to the ITCZ in the eastern Pacific. *Tellus A* **46,** 340–350 (1994).
7. Xie, S. P. *et al.* Global warming pattern formation: Sea surface temperature and rainfall. *J. Clim.* **23,** 966–986 (2010).
8. Bjerknes, J. Atmospheric teleconnections from the equatorial Pacific 1. *Mon. Weath. Rev.* **97,** 163–172 (1969).
9. Wang, C. An overlooked feature of tropical climate: Inter-Pacific-Atlantic variability. *Geophys. Res. Lett.* **33,** L12702 (2006).
10. Rodríguez-Fonseca, B. *et al.* Are Atlantic Niños enhancing Pacific ENSO events in recent decades? *Geophys. Res. Lett.* **36,** L20705 (2009).
11. England, M. *et al.* Recent intensification of wind-driven circulation in the Pacific and the ongoing warming hiatus. *Nature Clim. Change* **4,** 222–227 (2014).
12. Li, X., Holland, D. M., Gerber, E. P. & Yoo, C. Impacts of the north and tropical Atlantic Ocean on the Antarctic Peninsula and sea ice. *Nature* **505,** 538–542 (2014).
13. Lau, N. C. & Nath, M. J. A modeling study of the relative roles of tropical and extratropical SST anomalies in the variability of the global atmosphere-ocean system. *J. Clim.* **7,** 1184–1207 (1994).
14. Wallace, J. M. & Gutzler, D. S. Teleconnections in the geopotential height field during the Northern Hemisphere winter. *Mon. Weath. Rev.* **109,** 784–812 (1981).
15. Alexander, M. A. *et al.* The atmospheric bridge: The influence of ENSO teleconnections on air-sea interaction over the global oceans. *J. Clim.* **15,** 2205–2231 (2002).
16. Chang, P., Fang, Y., Saravanan, R., Ji, L. & Seidel, H. The cause of the fragile relationship between the Pacific El Niño and the Atlantic Niño. *Nature* **443,** 324–328 (2006).
17. Annamalai, H. S. P. X., Xie, S. P., McCreary, J. P. & Murtugudde, R. Impact of Indian Ocean sea surface temperature on developing El Niño. *J. Clim.* **18,** 302–319 (2005).
18. Kug, J. S., Kirtman, B. P. & Kang, I. S. Interactive feedback between ENSO and the Indian Ocean in an interactive ensemble coupled model. *J. Clim.* **19,** 6371–6381 (2006).
19. Keenlyside, N. S., Latif, M., Jungclaus, J., Kornblueh, L. & Roeckner, E. Advancing decadal-scale climate prediction in the North Atlantic sector. *Nature* **453,** 84–88 (2008).
20. Ham, Y. G., Kug, J. S., Park, J. Y. & Jin, F. F. Sea surface temperature in the north tropical Atlantic as a trigger for El Niño/Southern Oscillation events. *Nature Geosci.* **6,** 112–116 (2013).
21. Kucharski, F., Syed, F. S., Burhan, A., Farah, I. & Gohar, A. Tropical Atlantic influence on Pacific variability and mean state in the twentieth century in observations and CMIP5. *Clim. Dynam.* **44,** 881–896 (2015).
22. Booth, B. B., Dunstone, N. J., Halloran, P. R., Andrews, T. & Bellouin, N. Aerosols implicated as a prime driver of twentieth-century North Atlantic climate variability. *Nature* **484,** 228–232 (2012).
23. Schlesinger, M. E. & Ramankutty, N. An oscillation in the global climate system of period 65–70 years. *Nature* **367,** 723–726 (1994).
24. Zhang, R. & Delworth, T. L. A new method for attributing climate variations over the Atlantic Hurricane Basin's main development region. *Geophys. Res. Lett.* **36,** L06701 (2009).
25. Gill, A. Some simple solutions for heat-induced tropical circulation. *Q. J. R. Meteorol. Soc.* **106,** 447–462 (1980).
26. Vimont, D. J., Battisti, D. S. & Hirst, A. C. Footprinting: A seasonal connection between the tropics and mid-latitudes. *Geophys. Res. Lett.* **28,** 3923–3926 (2001).
27. Lee, S.-K. *et al.* Pacific origin of the abrupt increase in Indian Ocean heat content during the warming hiatus. *Nature Geosci.* **8,** 445–449 (2015).
28. Chikamoto, Y. *et al.* Skilful multi-year predictions of tropical trans-basin climate variability. *Nature Commun.* **6,** 6869 (2015).
29. Kucharski, F. *et al.* Atlantic forcing of Pacific decadal variability. *Clim. Dynam.* http://dx.doi.org/10.1007/s00382-015-2705-z (2015).
30. Zhang, R. & Delworth, T. L. Impact of the Atlantic multidecadal oscillation on North Pacific climate variability. *Geophys. Res. Lett.* **33,** L17712 (2006).

Acknowledgements

X.L. was supported by the Scripps Postdoctoral Fellowship; S.-P.X. was supported by the NSF grant AGS-1305719; S.T.G. was supported by the NSF grant OCE-1234473. C.Y. was supported by the Korea Meteorological Administration Research and Development Program under Grant KMIPA 2015–6110. The HadISST sea surface temperature (SST) data were provided by the British Met Office, Hadley Centre. The Kaplan SST and ERSST data sets were provided by the National Oceanic and Atmospheric Administration (NOAA) Earth System Research Laboratory. The Global Precipitation Climatology Project (GPCP) data were provided by the World Climate Research Programme's (WCRP) Global Energy and Water Exchanges Projects (GEWEX). Ishii subsurface temperature data were provided by the National Center for Atmospheric Research (NCAR) CISL Data Research Archive. The ERA-Interim atmospheric reanalysis was provided by the European Centre for Medium Range Weather Forecasts (ECMWF). We thank the WCRP Working Group on Coupled Modelling, which is responsible for the CMIP multi-model ensemble. The Community Earth System Model, CESM, and its atmospheric component, CAM4, were made available by NCAR, supported by the National Science Foundation (NSF) and the Office of Science (BER) of the US Department of Energy (DOE). The idealized atmospheric model, GFDL dry dynamical core, was developed by NOAA at the Geophysical Fluid Dynamics Laboratory (GFDL). Computing resources were provided by Yellowstone high-performance computing (HPC) in NCAR's Computational and Information Systems Laboratory, and by the HPC at New York University (NYU).

Author contributions

X.L., S.-P.X. and S.T.G. designed the experiments; X.L. performed the data analysis and numerical simulations, and prepared all figures; X.L. and C.Y. ran the CESM and GFDL simulations; all authors wrote and reviewed the manuscript.

Additional information

Supplementary information is available in the online version of the paper. Reprints and permissions information is available online at www.nature.com/reprints.
Correspondence and requests for materials should be addressed to X.L. or S.-P.X.

Competing financial interests

The authors declare no competing financial interests.

© 2016 Macmillan Publishers Limited. All rights reserved

Methods

Data sets. The UK Met Office Hadley Centre's SST data set HadISST (ref. 31) was employed in this study to estimate the trend of the tropical SST from 1979 to 2012 (Fig. 1a), and the SST trend over the tropical Atlantic estimated by this data set was used to force the CESM and CAM4 models. The Kaplan Extended SST version2 (ref. 32), and the National Oceanic and Atmospheric Administration (NOAA) Extended Reconstructed SST version 3b (ref. 33), were also used together with the HadISST to reveal the decadal relationship between the tropical Atlantic and the Indo-western Pacific.

The Ishii Subsurface Ocean Temperature Analysis[34] was used to calculate the subsurface ocean temperature trends from 1979 to 2012 (Fig. 1e). The Global Precipitation Climatology Project[35] (GPCP) data were used to estimate the trend in the tropical precipitation for the same period. The European Centre for Medium Range Weather Forecasts (ECMWF) Interim reanalysis[36] (ERA-Interim) data were used to estimate the trend in the atmospheric circulation (Fig. 1a,c).

Model results from the Coupled Model Intercomparison Project[37] (CMIP5) historical experiments were used to identify the relationship between the tropical Atlantic and the Indo-western Pacific decadal-mean SST.

Analyses methods. Sen's slope[38] method is used to calculate the observed trends, with the confidence intervals estimated using the Mann–Kendall test[39]. We used Student's t-test to calculate the confidence interval of the model responses.

CESM model experiments. The National Center for Atmospheric Research (NCAR) coupled climate model, the Community Earth System Model[40] (CESM1.06) was used in this study to investigate the response of the tropical climate system to an observed tropical Atlantic warming. We used F19_G16 (ref. 40) horizontal resolution, with ~2° resolution in the atmospheric component, and ~1° in the ocean component. We restored the tropical Atlantic temperature in the coupled model with an external heating within the mixed layer as follows:

$$F = cD(T_r - T_m)/\tau$$

where c is the heat content of sea water, D is the mixed-layer depth, T_r is the restoring target temperature, T_m is the model temperature at each time step, and τ is the restoring timescale, which was set as 20 days in this study.

The CESM response to the tropical Atlantic warming was calculated as the ensemble mean of 12 sensitivity experiments. In each experiment, we estimate the difference between a control run and a perturbed run. In the control run, the ocean temperature in the mixed layer of the tropical Atlantic (defined as the Atlantic Ocean between 20° S and 20° N, with linear buffer zones extending from 20° S to 30° S and from 20° N to 30° N) was restored to the model climatology. In the perturbed run, the tropical Atlantic SST was restored to the model climatology plus the observed 1979–2012 SST trend. We generated 12 ensemble members by slightly perturbing the external forcing around the observed SST trend (±0.1%, ±0.2%, ±0.6%, ±1%, ±1.4%, ±1.8% from the observed trend). Each simulation starts from the year-2000 initial condition of the CESM system and lasts for 30 model years. The first 5 years serve as a spin-up simulation and the results from year 6 to year 30 are used in the calculation. The ensemble mean of these simulations is then considered to be the CESM response to the observed trend of the tropical Atlantic SST.

CAM4 model simulations. The NCAR atmospheric model, the Community Atmosphere Model version 4 (CAM4), was used in this study to identify the tropical atmospheric responses to the Atlantic SST trend from 1979 to 2012. CAM4 is the atmospheric component of CESM and is run with the same resolution. As we do with the CESM simulation, we estimate the CAM4 response by differencing the control runs (with the climatological SST forcing) from the perturbed runs (forced by the tropical Atlantic SST trend).

GFDL dry-dynamical-core simulations. The spectral dry dynamical core of an atmospheric general circulation model[41], developed at the Geophysical Fluid Dynamics Laboratory (GFDL), was used to investigate the evolution of the atmospheric response to a tropical Atlantic warming, in a primitive-equation dynamical system. The idealized model is initialized with the climatological background flow from the ERA-Interim reanalysis, averaged from 1979 to 2012. At each time step, an additional forcing that balances the model's initial tendency associated with the climatological background flow was added to keep the model steady[42,43]. This external forcing ensures that the model response at each time step is due only to the initial tropical perturbation. In the forced cases, a convective heating is added as an initial impulse over the tropical Atlantic. The model results at each snapshot could be interpreted as the evolution of the primitive-equation dynamics in response to the tropical heating (see ref. 43 for details).

Surface heat flux and WES effect. The change of SST $\partial T'/\partial t$ satisfies a balance[5,6] between the oceanic dynamics D_o and four surface heat flux components: solar radiation Q_S, long-wave radiation Q_L, sensitive heat flux Q_H, and latent heat flux Q_E, which can be expressed as:

$$C\frac{\partial T'}{\partial t} = D_o + Q_S + Q_L + Q_H + Q_E \quad (1)$$

where C is the heat capacity of the upper ocean, up to the depth of interest.

The latent heat flux Q_E can be further decomposed into an atmospheric forcing term Q_E^a and an oceanic response term Q_E^o,

$$Q_E = Q_E^a + Q_E^o = \frac{\partial Q_E}{\partial W}W' + Q_E^r + \frac{\partial Q_E}{\partial T}T' \quad (2)$$

The former is mostly sensitive to the surface wind anomaly (W'), and the latter serves as a Newtonian damping with respect to the ocean temperature change (T'). Q_E^r refers to the residuals of the atmospheric forcing related to the relative humidity and stability effect and serves as a second-order factor[6] in this study.

When the surface wind is reduced, according to the bulk formula, the evaporation will be suppressed. This effect thus increases the latent heat flux from the atmosphere to the ocean, warming the sea surface[5].

References

31. Rayner, N. A. *et al.* Global analyses of sea surface temperature, sea ice, and night marine air temperature since the late nineteenth century. *J. Geophys. Res.* **108,** 4407 (2003).
32. Kaplan, A. *et al.* Analyses of global sea surface temperature 1856–1991. *J. Geophys. Res.* **103,** 18567–18589 (1998).
33. Smith, T. M. & Reynolds, R. W. Extended reconstruction of global sea surface temperatures based on COADS data (1854–1997). *J. Clim.* **16,** 1495–1510 (2003).
34. Ishii, M., Kimoto, M., Sakamoto, K. & Iwasaki, S. I. Steric sea level changes estimated from historical ocean subsurface temperature and salinity analyses. *J. Oceanogr.* **62,** 155–170 (2006).
35. Xie, P. *et al.* GPCP pentad precipitation analyses: An experimental dataset based on gauge observations and satellite estimates. *J. Clim.* **16,** 2197–2214 (2003).
36. Dee, D. P. *et al.* The ERA-Interim reanalysis: Configuration and performance of the data assimilation system. *Q. J. R. Meteorol. Soc.* **137,** 553–597 (2011).
37. Pirani, A. (ed) *WCRP Coupled Model Intercomparison Project—Phase 5—CMIP5* (*CLIVAR Exchanges* special issue No. 56, Vol. 16, May 2011); http://ensembles-eu.metoffice.com/cmug/CLIVAR_Exchange.pdf
38. Sen, P. K. Estimates of the regression coefficient based on Kendall's tau. *J. Am. Stat. Assoc.* **63,** 1379–1389 (1968).
39. Richard, O. G. *Statistical Methods for Environmental Pollution Monitoring* (Wiley, 1987).
40. Bretherton, C. S., Smith, C. & Wallace, J. M. An intercomparison of methods for finding coupled patterns in climate data. *J. Clim.* **5,** 541–560 (1992).
41. Held, I. M., Max, J. & Suarez, A. Proposal for the intercomparison of the dynamical cores of atmospheric general circulation models. *Bull. Am. Meteorol. Soc.* **75,** 1825–1830 (1994).
42. James, P. M., Fraedrich, K. & James, I. N. Wave-zonal-flow interaction and ultra-low frequency variability in a simplified global circulation model. *Q. J. R. Meteorol. Soc.* **120,** 1045–1067 (1994).
43. Yoo, C., Lee, S. & Feldstein, S. B. Arctic response to an MJO-like tropical heating in an idealized GCM. *J. Atmos. Sci.* **69,** 2379–2393 (2012).

© 2016 Macmillan Publishers Limited. All rights reserved